Computers Math. Applic. Vol. 22, No. 11, pp. 47–58, 1991
Printed in Great Britain.

0097-4943/91 $3.00 + 0.00

EXPLICIT THREE-POINT THREE-LEVEL FDMS FOR THE ONE-DIMENSIONAL CONSTANT-COEFFICIENT ADVECTION-DIFFUSION EQUATION

J. B. NIXON AND B. J. NOYE
Applied Mathematics Department, The University of Adelaide
GPO Box 498, Adelaide SA 5001, Australia

(Received February 1991)

Abstract—Two highly stable explicit three-point three-level finite difference methods for the one-dimensional constant-coefficient advection-diffusion equation are described. These are developed using differencing on a (1,3,1) computational stencil. One is conditionally stable with second-order accuracy, the other is conditionally stable with third-order accuracy. Both are free of numerical diffusion. The two methods are compared, theoretically and by means of numerical experiments, with the leapfrog/Du Fort-Frankel (1,2,1) explicit method, the only three-level method currently employed to solve this equation. The former are generally found to be more accurate than the latter.

INTRODUCTION

The one-dimensional advection-diffusion equation, used to describe the transport of passive scalars in a moving fluid, may be scaled and written in the form

$$\frac{\partial \hat{\tau}}{\partial t} + u\frac{\partial \hat{\tau}}{\partial x} - \alpha\frac{\partial^2 \hat{\tau}}{\partial x^2} = 0, \qquad 0 \le x \le 1, \quad 0 \le t \le T, \tag{1}$$

where $\hat{\tau}(x,t)$ may represent, for example, a pollutant concentration at position x and time t. In the following, u and α are considered to be positive constants quantifying the advection and diffusion processes, respectively.

Equation (1) has been used to describe transport in studies of: thermal pollution in river systems [1]; dispersion of dissolved salts in groundwater [2]; flow in porous media [3]; adsorption of chemicals into beds [4]; and dispersion of contaminants in estuaries and coastal seas [5].

The solution domain of the problem is covered by a mesh of grid-lines $t = n\,\Delta t$, $n = 0, 1, \ldots, N$, and $x = j\,\Delta x$, $j = 0, 1, \ldots, J$, parallel to the space and time coordinate axes, respectively. Approximations τ_j^n to $\hat{\tau}(j\,\Delta x, n\,\Delta t)$ are calculated at the point of intersection of these lines, namely, $(j\,\Delta x, n\,\Delta t)$ which is referred to as the (j,n) grid-point. The constant spatial and temporal grid-spacings are $\Delta x = 1/J$ and $\Delta t = T/N$, respectively. The approximation to the derivative $\frac{\partial^p \hat{\tau}(j\Delta x, n\Delta t)}{\partial x^p}$ is denoted $\frac{\partial^p \tau}{\partial x^p}\big|_j^n$.

A finite difference method (FDM) is termed a "p-level method" if the corresponding finite difference equation (FDE) involves grid-points at the p time-levels $(n+1)$, n, ..., $(n-p+2)$. A FDM is termed a "(k,l,m) method" if the FDE for the method involves k, l and m grid-points at the $(n+1)$, n and $(n-1)$ time-levels, respectively. A FDM is also termed a "q-point method" if the FDE has a computational stencil which has a spatial "spread" of q grid-points.

EQUIVALENT AND MODIFIED EQUIVALENT PDES

Consider the FDE

$$\mathcal{L}_\Delta[\tau_j^n] = 0, \tag{2}$$

which is consistent with the given partial differential equation (PDE) (1). The coefficients of the terms in the FDE (2) are functions of the Courant and diffusion numbers

$$c = \frac{u(\Delta t)}{(\Delta x)}, \quad s = \frac{\alpha(\Delta t)}{(\Delta x)^2}, \tag{3}$$

respectively. Expanding each term of the FDE (2) in Taylor series about the (j, n) grid-point yields the equivalent partial differential equation (EPDE)

$$\frac{\partial \tau}{\partial t} + u\frac{\partial \tau}{\partial x} - \alpha\frac{\partial^2 \tau}{\partial x^2} + E = 0, \tag{4}$$

in which

$$E = \sum_{p=2}^{\infty}\sum_{q=0}^{p} C_{q\,p-q}\,\frac{\partial^p \tau}{\partial x^q\,\partial t^{p-q}}. \tag{5}$$

The leading terms in E (called the truncation error of the FDE (2) relative to the PDE (1)) contain derivatives with respect to both space and time, and the magnitude of these terms indicate the order of accuracy of the resulting FDM. However, errors introduced through spatial discretization may cancel with errors introduced through temporal discretization. This is accounted for by considering the modified equivalent partial differential equation (MEPDE), found by converting all time derivatives in (5) into derivatives with respect to space [6]. An efficient computational procedure for achieving this is described in [7].

In this way it is found that all FDEs which are consistent with the PDE (1) have MEPDEs of the form (4), in which the truncation error E may be re-written

$$E = u\sum_{p=2}^{\infty}\frac{(\Delta x)^{p-1}}{p!}\eta_p(c,s)\frac{\partial^p \tau}{\partial x^p}. \tag{6}$$

A FDE (2) approximating the PDE (1) is termed "r^{th}-order accurate" if $\eta_p(c,s) = 0$, for $p = 2, 3, \ldots, r$ and $\eta_{r+1}(c,s) \neq 0$ in the corresponding MEPDE (4), (6). If $\eta_2(c,s) \neq 0$, the diffusion coefficient associated with the FDE is not α (as required for the correct solution of the PDE (1)) and the method is first-order accurate. Such a FDM is said to introduce numerical diffusion into the solution of the PDE (1).

CONVERGENCE, CONSISTENCY, STABILITY AND NON-NEGATIVITY

A FDM which approximates a given PDE is said to be convergent if, at each point in the solution domain, the finite difference solution approaches the exact solution in the limit as $\Delta x, \Delta t \to 0$. By the Lax equivalence theorem [8] a FDE which is consistent, in this limit, with a linear PDE involved in a well posed initial boundary value problem is convergent if and only if the FDE remains stable in the same limit. The von Neumann method of analysis [9] determines stability of a FDE governing transport of a scalar in just such a limit, whereas the frequently used matrix stability analysis [10] is based on a fixed temporal grid-spacing with the number of time iterations, N, tending to infinity. In order to use the equivalence theorem to ensure convergence, the former stability analysis is chosen.

Von Neumann stability analysis is based on the condition

$$|G(c,s,N_\lambda)| \leq 1 + O\{\Delta t\}, \qquad N_\lambda \geq 2, \tag{7}$$

where N_λ is the number of grid-spacings, Δx, in the wavelength, λ, of a component wave of $\hat{\tau}(x,0)$. The function G, the so called von Neumann amplification factor, is obtained by means of the substitution

$$\tau_j^n = (G)^n \exp\left\{i\left(\frac{2\pi j}{N_\lambda}\right)\right\}, \qquad i = \sqrt{-1}, \tag{8}$$

into the FDE (2). The FDM is stable if all the roots of the resulting polynomial in G are such that $|G(c,s,\beta)| \leq 1$ for all $\beta \in [0,2\pi]$, where $\beta = 2\pi/N_\lambda$. Criteria on the coefficients of the polynomial for this to be true are given in [11].

It is sometimes important that the numerical solution of a PDE and its associated initial and boundary conditions reflects a particular property of the exact solution of the system. For instance, when the PDE (1) is used to predict the spread of pollutants, it is essential for the predicted values to be either positive or zero—negative concentrations have no physical meaning. Clearly, an explicit FDE approximating a PDE with non-negative initial and boundary conditions will produce non-negative values if all the coefficients on the right-hand side of the explicit equation are themselves non-negative [12]. In the following, the region in the first quadrant of the c-s plane in which FDMs are non-negative, as well as von Neumann stable, will be determined.

WAVE PROPAGATION CHARACTERISTICS

As a means of estimating the accuracy of a FDM, an investigation of the changes to the amplitude and wave speed of an initial infinite travelling wave of unit amplitude which is propagating according to the PDE (1) is made. The amplitude response ζ, which is the ratio of the numerical amplitude a_N to the true amplitude a_T, after the wave has travelled one wavelength, together with the relative wave speed μ, which is the ratio of the numerical wave speed u_N to the true wave speed u, are parameters which indicate the accuracy of the FDE (2).

The coefficients of the truncation error terms of the MEPDE corresponding to a FDE are related to ζ and μ as follows [13]. The amplitude response $\zeta = a_N/a_T$, given in terms of G, is

$$\zeta(c,s,N_\lambda) = |G(c,s,N_\lambda)|^{N_\lambda/c} \exp\left\{\frac{4\pi^2 s}{cN_\lambda}\right\}, \tag{9}$$

while in terms of the $\eta_p(c,s)$ functions in the MEPDE (4), (6), it is given by

$$\zeta(c,s,N_\lambda) = \exp\left\{2\pi \sum_{r=1}^{\infty} \frac{(-1)^{r+1}}{(2r)!}\left(\frac{2\pi}{N_\lambda}\right)^{2r-1} \eta_{2r}(c,s)\right\}. \tag{10}$$

The relative wave speed $\mu = u_N/u$, given in terms of G, is

$$\mu(c,s,N_\lambda) = -\frac{N_\lambda}{2\pi c} \arg\{G(c,s,N_\lambda)\}, \tag{11}$$

while in terms of the $\eta_p(c,s)$ functions in the MEPDE (4), (6), it is given by

$$\mu(c,s,N_\lambda) = 1 + \sum_{r=1}^{\infty} \frac{(-1)^r}{(2r+1)!}\left(\frac{2\pi}{N_\lambda}\right)^{2r} \eta_{2r+1}(c,s), \tag{12}$$

in which arg is the argument of the complex variable. From Equations (10) and (12), it is clear that the error in modelling wave amplitude is associated with even-order derivatives in the MEPDE, and that the error in modelling wave speed is associated with odd-order derivatives. Note that Equations (10) and (12) only hold for large N_λ—clearly $\zeta \to 1$ and $\mu \to 1$ as $N_\lambda \to \infty$. In particular, ζ and μ approach unity faster for high-order than for low-order methods.

In obtaining the wave propagation graphs for each method considered, values of the amplitude response and relative wave speed for the FDM under discussion were obtained by application of Equations (9) and (11), respectively. Once these were obtained, the value of N_1, the greatest number of grid-spacings per wavelength below which there was an error of more than 1% in the respective wave propagation parameter ζ or μ, was obtained and graphs of N_1 against s for values of c within the appropriate stability region were then plotted.

A WEIGHTED (1,3,1) METHOD

On a spatially centred (1,3,1) computational stencil a combination of backward time (BT), forward time (FT) and centred time (CT) approximations may be used for the temporal derivative in the PDE (1). There are also three possible and similarly denoted standard approximations for the first spatial derivative, namely BS, FS and CS. Only two of the three approximations in time or space need to be used to discretize a given derivative however, since the third is a linear combination of the other two.

Using weights θ and ϕ in the following manner,

$$\left.\frac{\partial \hat{\tau}}{\partial t}\right|_j^n \approx \theta \times [\mathrm{BT}] + (1-\theta) \times [\mathrm{CT}], \quad \left.\frac{\partial \hat{\tau}}{\partial x}\right|_j^n \approx \phi \times [\mathrm{BS}] + (1-\phi) \times [\mathrm{CS}], \tag{13}$$

for the first-order derivatives and the standard CS approximation for the second spatial derivative in the PDE (1), yields the FDE

$$\tau_j^{n+1} = \frac{1}{[1-\theta]} [\{2s + c(1+\phi)\}\tau_{j-1}^n - 2\{2s + c\phi + \theta\}\tau_j^n + \{2s - c(1-\phi)\}\tau_{j+1}^n + \{1+\theta\}\tau_j^{n-1}], \tag{14}$$

which has a MEPDE of the general form (4), (6), with

$$\eta_2(c,s) = -(\phi + \theta c), \quad \eta_3(c,s) = 1 - c^2 + 3\theta\,(2s + c\,(\phi + \theta c)), \ldots. \tag{15}$$

THE LEAPFROG/DU FORT-FRANKEL (1,2,1) METHOD

The leapfrog/Du Fort-Frankel [14] spatially centred (1,2,1) explicit FDE

$$\tau_j^{n+1} = \frac{1}{[1+2s]} [\{c + 2s\}\tau_{j-1}^n - \{c - 2s\}\tau_{j+1}^n + \{1 - 2s\}\tau_j^{n-1}], \tag{16}$$

may be obtained by substituting

$$\theta = -2s, \quad \phi = 0, \tag{17}$$

into the FDE (14). Equation (16) is von Neumann stable in the region [15]

$$0 < c \leq 1, \quad s > 0, \tag{18}$$

shown horizontally shaded in Figure 1.

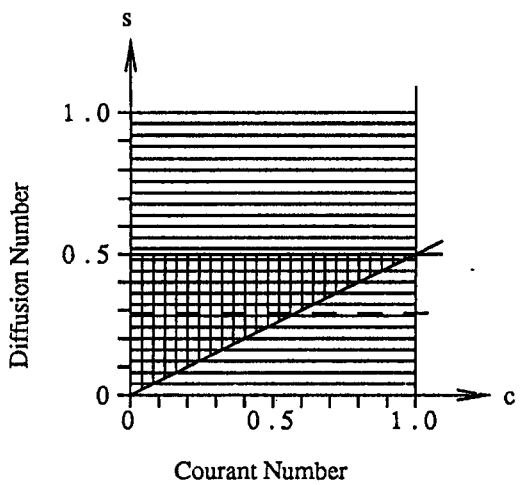

Figure 1. Regions of von Neumann stability (horizontally shaded) and non-negativity (vertically shaded) in the c-s plane for the first-order leapfrog/Du Fort-Frankel (1,2,1) FDE (16).

Approximations to the PDE (1) with non-negative initial and boundary conditions produced by the FDE (16) are guaranteed to be non-negative in the region defined by Equation (18) and

$$\frac{c}{2} \leq s \leq \frac{1}{2}, \tag{19}$$

shown vertically shaded in Figure 1.

This FDM has a MEPDE of the general form (4), (6), with

$$\eta_2(c,s) = 2cs, \quad \eta_3(c,s) = (1-c^2)(1-12s^2), \ldots, \tag{20}$$

indicating that the diffusion coefficient associated with this FDM is $\alpha(1-c^2)$, and that the method is first-order accurate and introduces numerical anti-diffusion for all c and s given by Equation (18).

Substituting Equation (20) into Equation (10), it is seen that for fixed positive c and s,

$$\zeta(c,s,N_\lambda) \to 1(+), \quad \text{as } N_\lambda \to \infty. \tag{21}$$

This implies that the component waves in the initial condition are propagated by the FDE (16) with an amplitude which is larger than when they are propagated by the PDE (1).

By substitution of Equation (20) into Equation (12), it is also seen that

$$\mu(c,s,N_\lambda) \to 1(\pm), \qquad \text{for } 0 < c < 1 \text{ and } s \gtrless 1/\sqrt{12}, \quad \text{as } N_\lambda \to \infty, \tag{22}$$

and that for $c = 1$ or $s = 1/\sqrt{12}$, the limit is approached more rapidly than for other values of c and s. In the limit, for values of c and s above the dashed line in Figure 1, the wave speed is overestimated by this method, while for values below this line it is underestimated.

Figure 2 shows graphs of N_1 against s for both amplitude response and relative wave speed with various values of c. Note that the curves for $c = 0.8$ and 1.0 in the wave amplitude graph almost coincide. In the wave speed graph, the curves for $c = 0.1$ and 0.2 almost coincide and the curve for $c = 1$ coincides with the s axis. These graphs indicate that small values of c and/or s result in much better approximations to the amplitude response than do large values of either parameter, and that the relative wave speed is indeed close to ideal for c near unity and s near $1/\sqrt{12} \approx 0.29$.

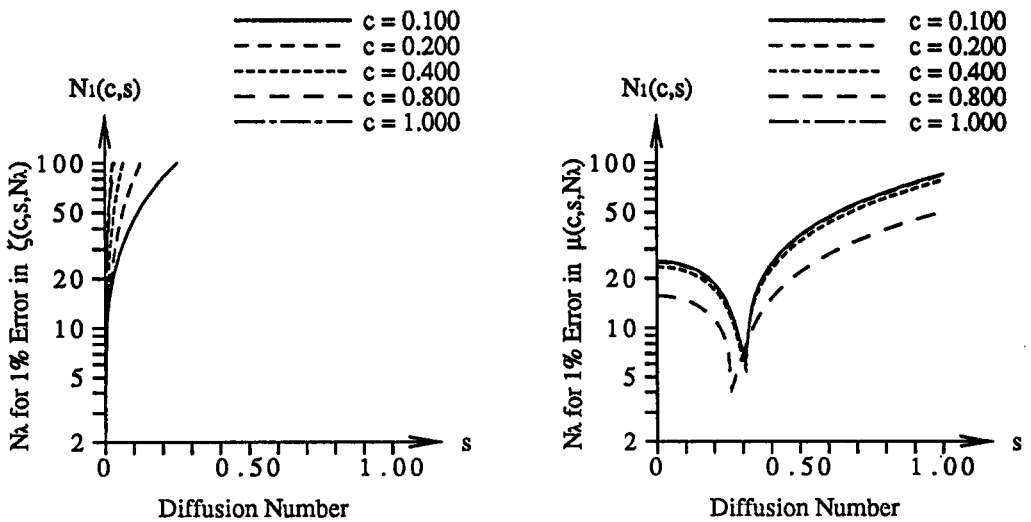

Figure 2. $N_1(c,s)$ for amplitude response and relative wave speed against s with various c, for the first-order leapfrog/Du Fort-Frankel (1,2,1) FDE (16).

THE OPTIMAL (1,2,1) METHOD

A FDM with no numerical diffusion, involving grid-points on the same spatially centred (1,2,1) computational stencil as the leapfrog/Du Fort-Frankel (1,2,1) method can be derived in the following manner. Setting

$$\theta = -(2s + c\,\phi) \tag{23}$$

in the FDE (14) removes the (j, n) grid-point from the set of those being considered. Setting

$$\phi = -\theta\, c \tag{24}$$

in Equation (15) ensures the method is second-order accurate and free of numerical diffusion. Substitution of Equations (23), (24) into the FDE (14) yields the (1,2,1) FDE

$$\tau_j^{n+1} = \frac{1}{[1 - c^2 + 2s]} \left[\{c(1 - c^2) + 2s\}\, \tau_{j-1}^n - \{c(1 - c^2) - 2s\}\, \tau_{j+1}^n + \{1 - c^2 - 2s\}\, \tau_j^{n-1}\right]. \tag{25}$$

The second-order FDE (25) is von Neumann stable in the region

$$0 < c \leq 1, \quad s > 0, \tag{26}$$

shown horizontally shaded in Figure 3.

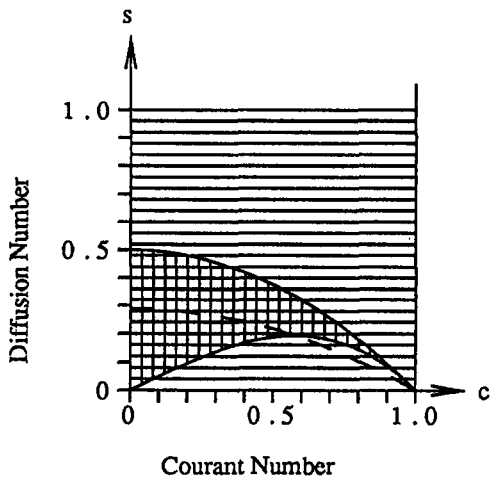

Figure 3. Regions of von Neumann stability (horizontally shaded) and non-negativity (vertically shaded) in the c-s plane for the second-order optimal (1,2,1) FDE (25).

It should be noted that on setting $s = 0$ in either the FDE (16) or the FDE (25), one obtains the leapfrog FDE for approximating the pure advection equation, and on setting $c = 0$ in either FDE, one obtains the Du Fort-Frankel FDE for approximating the pure diffusion equation.

The region in which the FDE (25) produces only non-negative values is given by Equation (26) and

$$\frac{c}{2}(1 - c^2) \leq s \leq \frac{1}{2}(1 - c^2), \tag{27}$$

shown vertically shaded in Figure 3.

This FDM has a MEPDE of the general form (4,6) with

$$\begin{aligned} \eta_2(c, s) &= 0, \\ \eta_3(c, s) &= 1 - c^2 - 12s^2(1 - c^2)^{-1}, \\ \eta_4(c, s) &= 2s\, c^{-1}\left(9c^2 - 1 + 12s^2(1 - 5c^2)(1 - c^2)^{-2}\right), \ldots . \end{aligned} \tag{28}$$

This is the optimal (highest order) FDM for the PDE (1) based on the spatially centred (1,2,1) computational stencil.

The dominant error in the use of the FDE (25) is third-order and involves the representation of wave speed. Using Equations (12), (26) and (28) it can be shown that

$$\mu(c, s, N_\lambda) \to 1(\pm), \qquad \text{for } s \gtrless \frac{1}{\sqrt{12}}(1-c^2), \quad \text{as } N_\lambda \to \infty. \tag{29}$$

Hence, for large N_λ and values of c and s above the dashed curve in Figure 3, the wave speed is overestimated by this method, while for values below this curve it is underestimated.

Figure 4 shows graphs of N_1 against s with various c for the wave propagation characteristics of this method. Note that the curve for $c = 1$ coincides with the s axis in the wave speed graph. Local minima in N_1 for amplitude response occur when $(c, s) \approx (0.1, 0.28)$, $(0.2, 0.25)$, $(0.8, 0.15)$ and $(1, 0)$. Local minima in N_1 for relative wave speed occur when $(c, s) \approx (0.1, 0.29)$, $(0.2, 0.28)$, $(0.4, 0.24)$ and $(0.8, 0.10)$, while the wave speed is ideal for $c = 1$, $s > 0$. Since the dominant error for this FDM is associated with wave speed, values of s close to those listed here would be expected to yield minimum errors in any numerical tests made with these values of c.

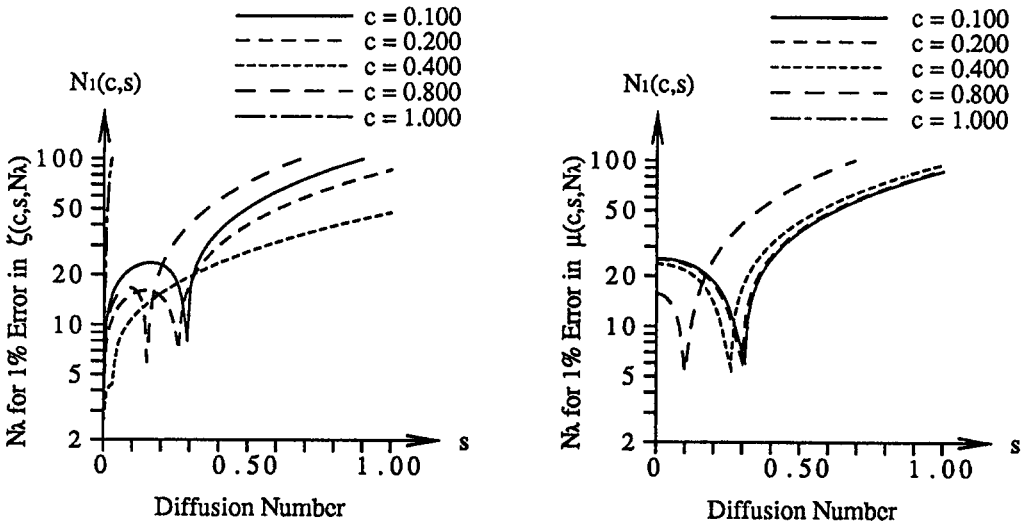

Figure 4. $N_1(c, s)$ for amplitude response and relative wave speed against s, with various c, for the second-order optimal (1,2,1) FDE (25).

THE OPTIMAL (1,3,1) METHOD

Choosing θ and ϕ to force $\eta_2(c, s) = \eta_3(c, s) = 0$ in Equation (15), yields

$$\theta = \frac{-(1-c^2)}{6s}, \qquad \phi = \frac{c(1-c^2)}{6s}, \tag{30}$$

which, on substitution into the FDE (14), gives the (1,3,1) FDE

$$\begin{aligned} \tau_j^{n+1} = \frac{1}{[1-c^2+6s]} \Big[&\{c^2(1-c^2) + 6s\,(2s+c)\}\,\tau_{j-1}^n + 2\{(1-c^2)^2 - 12s^2\}\,\tau_j^n \\ &+ \{c^2(1-c^2) + 6s\,(2s-c)\}\,\tau_{j+1}^n - \{1-c^2-6s\}\,\tau_j^{n-1} \Big]. \end{aligned} \tag{31}$$

This is the optimal FDM for the PDE (1) based on the spatially centred (1,3,1) computational stencil.

The horizontally shaded area of Figure 5 shows the von Neumann stability region for this method, namely

$$0 < c \leq 1, \quad 0 < s \leq \frac{1}{\sqrt{12}}(1-c^2). \tag{32}$$

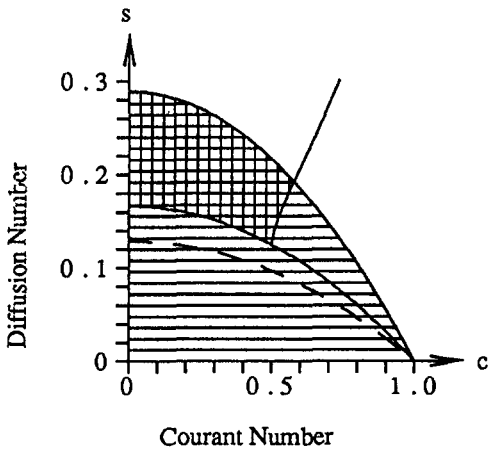

Figure 5. Regions of von Neumann stability (horizontally shaded) and non-negativity (vertically shaded) in the c-s plane for the third-order optimal (1,3,1) FDE (31).

The region in which the FDE (31) produces only non-negative values is given by Equation (32) and

$$\begin{aligned} &0 < s \leq \frac{1}{\sqrt{12}}(1-c^2), && \text{for } 0 < c \leq 1, \\ &s \geq \frac{1}{6}(1-c^2), && \text{for } 0 < c \leq 1, \\ &s \geq \frac{c}{12}\left[3-\sqrt{3(4c^2-1)}\right], && \text{for } \frac{1}{2} \leq c \leq 1. \end{aligned} \tag{33}$$

The region thus defined is shown vertically shaded in Figure 5.

This FDM has a MEPDE of the general form (4), (6) with

$$\begin{aligned} &\eta_2(c,s) = \eta_3(c,s) = 0, \\ &\eta_4(c,s) = 10cs - \frac{c(1-c^2)^2}{(6s)}, \\ &\eta_5(c,s) = (1+6c^2)(1-c^2) - 60s^2 - \frac{5c^2(1-c^2)^3}{(36s^2)}, \ldots . \end{aligned} \tag{34}$$

The dominant error in the use of the FDE (31) is fourth-order and involves the representation of wave amplitude. Using Equations (10) and (34), it can be shown that, for $s > 0$,

$$\zeta(c,s,N_\lambda) \to 1(\pm), \qquad \text{for } 0 < c \leq 1 \text{ and } s \lesssim \frac{1}{\sqrt{60}}(1-c^2), \quad \text{as } N_\lambda \to \infty. \tag{35}$$

Hence, for large N_λ and values of c and s above the dashed curve in Figure 5, the amplitude is underestimated by this method, while for values below this curve it is overestimated.

Figure 6 shows graphs of N_1 against s with various c for the wave propagation characteristics of this method. Local minima in N_1 for amplitude response occur when $(c,s) \approx (0.1,0.13)$, $(0.2,0.12)$, $(0.4,0.11)$ and $(0.8,0.05)$. Since the dominant error for this FDM is associated with wave amplitude, values of s close to those listed here would be expected to yield minimum errors in any numerical tests made with these values of c. Local minima in N_1 occur for relative wave speed when $(c,s) \approx (0.1,0.04)$, $(0.2,0.08)$, $(0.8,0.05)$ and $(1,0)$, and when $(c,s) \approx (0.1,0.13)$ and $(0.2,0.12)$.

A NUMERICAL TEST

Equation (1) has an exact solution

$$\hat{\tau}(x,t) = \frac{\sigma}{\sqrt{\sigma^2+2\alpha t}} \exp\left\{-\frac{(x-x_0-ut)^2}{2(\sigma^2+2\alpha t)}\right\}, \tag{36}$$

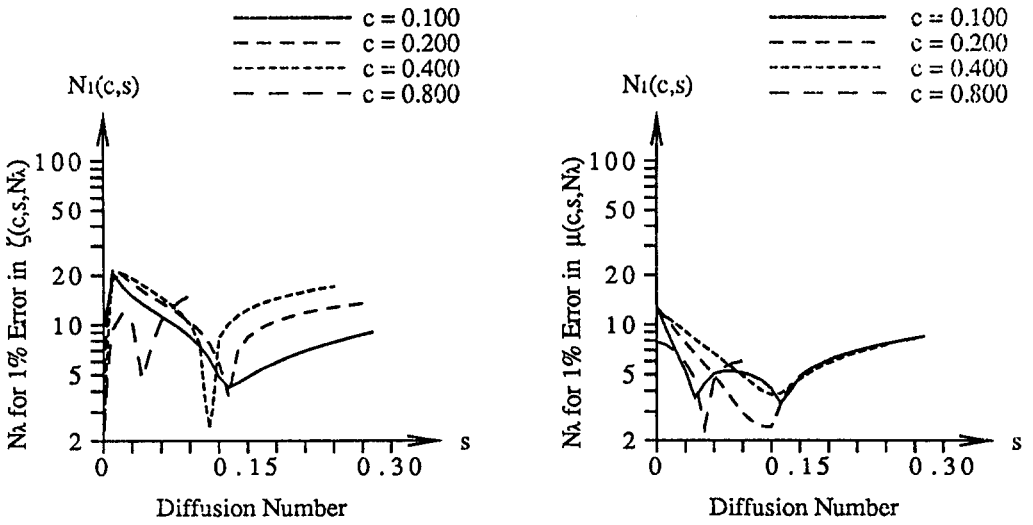

Figure 6. $N_1(c, s)$ for amplitude response and relative wave speed against s, with various c, for the third-order optimal (1,3,1) FDE (31).

for boundary conditions described by Equation (36) with $x = 0$ and 1, for $t \geq 0$, and an initial condition described by Equation (36) with $t = 0$, for $0 \leq x \leq 1$. The initial condition is a Gauss distribution centred at $x = x_0$ with unit pulse height and standard deviation of σ.

The FDEs (16), (25) and (31) for the leapfrog/Du Fort-Frankel (DF) (1,2,1), optimal (OPT) (1,2,1) and optimal (OPT) (1,3,1) methods, respectively, were used to approximate the PDE (1) with exact solution (36), using various values for c and s.

The parameters used for all tests were $u = 1.0$, $T = 1.0$, $x_0 = -0.5$, $\sigma = 0.025$, $\Delta x = 0.01$ ($J = 100$). Tests were carried out for five values of the cell Reynolds number $R_\Delta = c/s$, namely $R_\Delta = 1$ ($\alpha = 0.01$), 2 (0.005), 4 (0.0025), 8 (0.00125) and 16 (0.000625). For each value of R_Δ, four values of c were used, namely $c = 0.1$, 0.2, 0.4, and 0.8. For the four tests for each value of R_Δ, s was chosen to force $\Delta t = 0.001$ ($N = 1000$), 0.002 (500), 0.004 (250), 0.008 (125) as the value of c was increased. Equation (36) was used to produce values for the first time-level.

The theoretical accuracy (Order), average absolute error (Av{|Err|}) and minimum value of τ (Min{τ}) over all grid-points at the final time-level, and the central processor unit (CPU) time used, are listed in Table 1 for the parameter values resulting in stable tests of each method. Entries for Min{τ} which are in bold correspond to tests for which the FDE had non-negative coefficients. Values of magnitude $< 10^{-9}$ were considered insignificant. All computations were carried out in double precision on a Pyramid 9820 computer.

The results obtained show that the first-order DF(1,2,1) method is never more accurate than the second-order OPT(1,2,1) method for the values of c and s used. For small values of both these parameters, the methods produced errors of similar magnitude; for example, with $(c, s) = (0.1, 0.025)$, the average error is 1.79×10^{-3} for both methods. However, when c is large the second-order method produced much more accurate results than the first-order method; for example, with $(c, s) = (0.8, 0.1)$, the average error for the first-order method is 8.67×10^{-3} while it is about one thirtieth of this for the second-order method (2.61×10^{-4}).

Inspection of the table shows that the size of the average error obtained is closely related to the size of the dominant error term in the MEPDE of the method used. For the second-order OPT(1,2,1) method, this error is minimized by values of (c, s) on the dashed line in Figure 3. This corresponds to values of (c, s) at which N_1 for relative wave speed is a minimum in Figure 4. These theoretical results are illustrated by the errors listed in Table 1. For example, when $c = 0.4$, the minimum error predicted theoretically occurs when $s = 0.24$ for this method; of the errors tabulated for this c, the smallest (1.86×10^{-4}) occurs when $s = 0.2$. When $c = 0.8$, the smallest error of those listed (2.61×10^{-4}) occurs when $s = 0.1$, which is as predicted theoretically.

For all methods, tests with $R_\Delta = 1$, 2, and 4, produced no significant negative values. For the first- and second-order methods with $R_\Delta = 1$ and 2 ($c \neq 0.8$) this is expected, as the coefficients on the right-hand side of the FDEs are non-negative. For all methods tested with $R_\Delta = 4$, for

the OPT(1,2,1) method with $(R_\Delta, c) = (2, 0.8)$, and for the DF(1,2,1) and OPT(1,2,1) methods with $(R_\Delta, c) = (1, 0.8)$, the results contained no negatives even though some of the coefficients were negative; that is the positive coefficients (multiplied by the appropriate value of τ_j^n) were sufficiently large to prevent any result being negative. For $R_\Delta = 8$ no negative values were produced by the OPT(1,3,1) method, while negative values of the order of $\approx 10^{-8}$ were produced by the other two methods; for $R_\Delta = 16$ only the third-order method was non-negative, while negative values of the order of $\approx 10^{-2}$ appeared for $c = 0.1$, 0.2 and 0.4 for the first- and second-order methods, and approximately 10^{-6} and 10^{-7}, respectively, for $c = 0.8$.

Table 1. Numerical test results.

R_Δ	c	s	Method	Order	Av{|Err|}	Min{τ}	CPU
1	0.1	0.1	DF(1,2,1)	1	2.32×10^{-4}	0.0	2.80 sec
			OPT(1,2,1)	2	2.14×10^{-4}	0.0	2.68 sec
			OPT(1,3,1)	3	5.04×10^{-7}	0.0	2.83 sec
	0.2	0.2	DF(1,2,1)	1	5.44×10^{-4}	0.0	1.37 sec
			OPT(1,2,1)	2	1.13×10^{-4}	0.0	1.48 sec
			OPT(1,3,1)	3	1.96×10^{-6}	0.0	1.32 sec
	0.4	0.4	DF(1,2,1)	1	2.32×10^{-3}	0.0	0.68 sec
			OPT(1,2,1)	2	3.57×10^{-4}	0.0	0.70 sec
	0.8	0.8	DF(1,2,1)	1	1.10×10^{-2}	0.0	0.33 sec
			OPT(1,2,1)	2	5.06×10^{-3}	0.0	0.28 sec
2	0.1	0.05	DF(1,2,1)	1	6.64×10^{-4}	0.0	2.92 sec
			OPT(1,2,1)	2	6.63×10^{-4}	0.0	2.67 sec
			OPT(1,3,1)	3	8.64×10^{-6}	0.0	2.75 sec
	0.2	0.1	DF(1,2,1)	1	7.36×10^{-4}	0.0	1.43 sec
			OPT(1,2,1)	2	5.76×10^{-4}	0.0	1.27 sec
			OPT(1,3,1)	3	3.35×10^{-6}	0.0	1.32 sec
	0.4	0.2	DF(1,2,1)	1	2.25×10^{-3}	0.0	0.67 sec
			OPT(1,2,1)	2	1.86×10^{-4}	0.0	0.67 sec
			OPT(1,3,1)	3	1.77×10^{-5}	0.0	0.67 sec
	0.8	0.4	DF(1,2,1)	1	1.06×10^{-2}	0.0	0.30 sec
			OPT(1,2,1)	2	3.39×10^{-3}	0.0	0.33 sec
4	0.1	0.025	DF(1,2,1)	1	1.79×10^{-3}	0.0	2.68 sec
			OPT(1,2,1)	2	1.79×10^{-3}	0.0	2.87 sec
			OPT(1,3,1)	3	7.01×10^{-5}	0.0	2.73 sec
	0.2	0.05	DF(1,2,1)	1	1.74×10^{-3}	0.0	1.35 sec
			OPT(1,2,1)	2	1.69×10^{-3}	0.0	1.40 sec
			OPT(1,3,1)	3	5.75×10^{-5}	0.0	1.33 sec
	0.4	0.1	DF(1,2,1)	1	2.40×10^{-3}	0.0	0.72 sec
			OPT(1,2,1)	2	1.27×10^{-3}	0.0	0.75 sec
			OPT(1,3,1)	3	7.96×10^{-6}	0.0	0.65 sec
	0.8	0.2	DF(1,2,1)	1	9.83×10^{-3}	0.0	0.35 sec
			OPT(1,2,1)	2	1.77×10^{-3}	0.0	0.33 sec
8	0.1	0.0125	DF(1,2,1)	1	4.36×10^{-3}	-6.4×10^{-8}	2.58 sec
			OPT(1,2,1)	2	4.35×10^{-3}	-5.7×10^{-8}	2.77 sec
			OPT(1,3,1)	3	4.37×10^{-4}	0.0	2.63 sec
	0.2	0.025	DF(1,2,1)	1	4.25×10^{-3}	-5.5×10^{-8}	1.30 sec
			OPT(1,2,1)	2	4.19×10^{-3}	-3.0×10^{-8}	1.30 sec
			OPT(1,3,1)	3	4.00×10^{-4}	0.0	1.35 sec
	0.4	0.05	DF(1,2,1)	1	4.02×10^{-3}	-6.6×10^{-9}	0.68 sec
			OPT(1,2,1)	2	3.55×10^{-3}	0.0	0.68 sec
			OPT(1,3,1)	3	2.56×10^{-4}	0.0	0.62 sec
	0.8	0.1	DF(1,2,1)	1	8.67×10^{-3}	0.0	0.32 sec
			OPT(1,2,1)	2	2.61×10^{-4}	0.0	0.40 sec
			OPT(1,3,1)	3	2.33×10^{-4}	0.0	0.32 sec
16	0.1	0.00625	DF(1,2,1)	1	9.37×10^{-3}	-1.4×10^{-2}	2.57 sec
			OPT(1,2,1)	2	9.36×10^{-3}	-1.3×10^{-2}	2.78 sec
			OPT(1,3,1)	3	1.80×10^{-3}	0.0	2.75 sec
	0.2	0.0125	DF(1,2,1)	1	9.10×10^{-3}	-1.3×10^{-2}	1.30 sec
			OPT(1,2,1)	2	9.06×10^{-3}	-1.2×10^{-2}	1.37 sec
			OPT(1,3,1)	3	1.71×10^{-3}	0.0	1.32 sec
	0.4	0.025	DF(1,2,1)	1	8.27×10^{-3}	-9.7×10^{-3}	0.72 sec
			OPT(1,2,1)	2	7.86×10^{-3}	-6.9×10^{-3}	0.70 sec
			OPT(1,3,1)	3	1.34×10^{-3}	0.0	0.67 sec
	0.8	0.05	DF(1,2,1)	1	7.67×10^{-3}	-9.8×10^{-5}	0.33 sec
			OPT(1,2,1)	2	2.69×10^{-3}	-3.8×10^{-7}	0.35 sec
			OPT(1,3,1)	3	5.91×10^{-5}	0.0	0.33 sec

When the results obtained for the third-order OPT(1,3,1) method are compared with those of the second-order OPT(1,2,1) method, the average error of the former is generally found to be

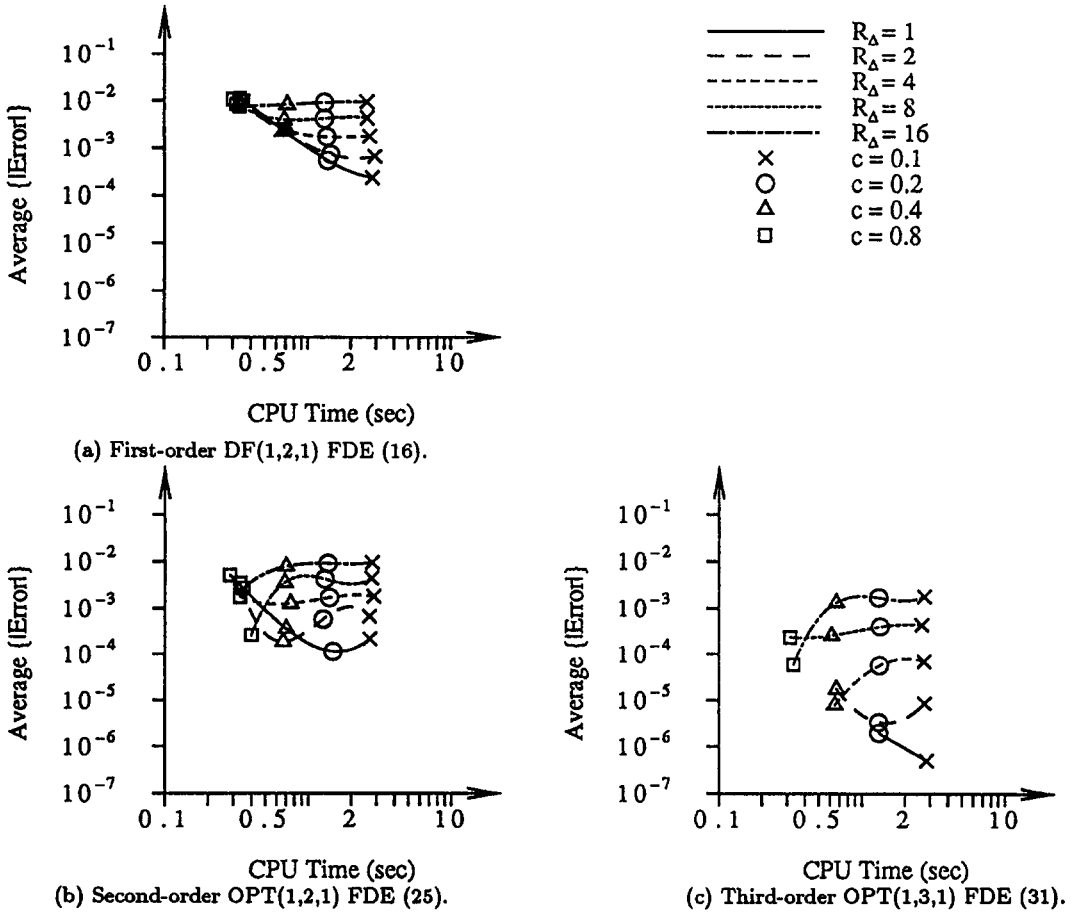

(a) First-order DF(1,2,1) FDE (16).

(b) Second-order OPT(1,2,1) FDE (25).

(c) Third-order OPT(1,3,1) FDE (31).

Figure 7. Average {|Error|} graphed against CPU.

at least one order of magnitude smaller than the latter, for $R_\Delta \leq 8$. Results for the third-order method are most accurate when R_Δ and c are both small; for instance, for $(R_\Delta, c) = (1, 0.1)$, the method produces an average error $\approx 1/400$ of those of the first- and second-order methods, and for $(R_\Delta, c) = (1, 0.2)$, $(2, 0.1)$ and $(2, 0.2)$, it produces an average error $\approx 1/75$ of those of the other two methods.

For the OPT(1,3,1) method, the magnitude of errors illustrates the theoretical findings observed in Figures 5 and 6, with smallest errors generally occurring for values of (c, s) minimizing the dominant error term in the MEPDE (34). For instance, when $c = 0.4$ the theoretical optimum value of the diffusion number is $s = 0.11$, while of the values tested the smallest error (7.96×10^{-6}) occurred for $s = 0.1$.

No significant negative values appeared in the results of all numerical tests applied to the OPT(1,3,1) method even though the parameters used did not always lie in the region of the c-s plane in which the coefficients of the FDE (31) were all non-negative.

In order to determine the efficiency of these methods based on assessment of accuracy relative to central processor unit (CPU) time required, graphs of average absolute error (Average{|Error|}) against CPU time used are plotted for each method in Figure 7. The graphs show certain common features. For example, the CPU time required for a run with a given value of c is almost independent of the value of R_Δ used, and this time increases with increasing c. In fact there was little difference in the CPU time required by each of the methods when the parameters used were the same. For instance, with $(R_\Delta, c) = (2, 0.4)$, all three methods required 0.67 sec. This property is due to the fact that the number of time levels, N, and space steps, J, involved are the same for a given pair of R_Δ and c.

For the first-order DF(1,2,1) method (see Figure 7(a)), average errors ranged from 2.32×10^{-4} to 1.06×10^{-2} while CPU time ranged from 0.30 to 2.92 sec. For $c = 0.8$ the errors and CPU time are practically independent of R_Δ (or s), and as c decreases more accurate results are obtained

using the same CPU time with smaller values of R_Δ. There appears to be no obviously optimal value of (R_Δ, c) for which both error and CPU time are small.

For the second-order OPT(1,2,1) method (see Figure 7(b)) the errors and the CPU times ranged over approximately the same values as those for the first-order method. However, when the results for $c = 0.8$, which required the least CPU time, are examined it is clear that $R_\Delta = 8$ is optimal, producing an average error of 2.61×10^{-4} in only 0.40 sec. This may be compared with, for example, the similar error of 2.14×10^{-4} produced in 2.68 sec when $(R_\Delta, c) = (1, 0.1)$.

Results for the third-order OPT(1,3,1) method are shown in Figure 7(c). For the same CPU times as those for the first- and second-order methods, the errors produced are clearly much smaller. Although there is no obviously optimal value of (R_Δ, c) for maximum efficiency, this method is clearly superior to the other two. For instance, the choice of $(R_\Delta, c) = (16, 0.8)$ produces an average error of 5.91×10^{-5} in only 0.33 sec compared with the most efficient case for the second-order OPT(1,2,1) method, namely an average error of 2.61×10^{-4} in 0.40 sec with the choice $(R_\Delta, c) = (8, 0.8)$.

CONCLUSION

In general, the second-order (1,2,1) method was not significantly more accurate than the first-order leapfrog/Du Fort-Frankel method, while the new third-order (1,3,1) method was at least an order of magnitude more accurate than either of these. This arises as a consequence of the absence of low-order errors in wave speed for the latter method and the presence of these errors for the former methods. The second-order method is to be preferred over the first-order method for moderate cell Reynolds numbers of the order of 10. The third-order method, while more restrictive with respect to stability, clearly results in smaller errors for comparable CPU times when compared with the two lower order methods.

REFERENCES

1. M.H. Chaudhry, D.E. Cass and J.E. Edinger, Modelling of unsteady-flow water temperatures, *Journal of Hydraulic Engineering* **109** (5), 657–669 (1983).
2. V. Guvanasen and R.E. Volker, Numerical solutions for solute transport in unconfined aquifers, *International Journal for Numerical Methods in Fluids* **3** (2), 103–123 (1983).
3. N. Kumar, Unsteady flow against dispersion in finite porous media, *Journal of Hydrology* **63** (3/4), 345–358 (1983).
4. L. Lapidus and N.R. Amundson, Mathematics of adsorption in beds, VI: The effect of longitudinal diffusion in ion exchange and chromatographic columns, *The Journal of Physical Chemistry* **56** (8), 984–988 (1952).
5. B.J. Noye, Numerical methods for solving the transport equation, In *Numerical Modelling: Applications to Marine Systems*, pp. 195–229, North-Holland Mathematics Studies, Elsevier Science Publishers B.V. (North-Holland), Amsterdam, (1987).
6. R.F. Warming and B.J. Hyett, The modified equation approach to the stability and accuracy analysis of finite-difference methods, *Journal of Computational Physics* **14** (2), 159–179 (1974).
7. B.J. Noye and K. Hayman, Accurate finite difference methods for solving the advection-diffusion equation, In *Computational Techniques and Applications: CTAC-85*, pp. 137–157, Elsevier Science Publishers B.V. (North-Holland), Amsterdam, (1986).
8. P.D. Lax and R.D. Richtmyer, Survey of the stability of linear finite-difference equations, *Communications on Pure and Applied Mathematics* **9** (2), 267–293 (1956).
9. G.G. O'Brien, M.A. Hyman and S. Kaplan, A study of the numerical solution of partial differential equations, *Journal of Mathematics and Physics* **29**, 223–251 (1950).
10. G.D. Smith, *Numerical Solution of Partial Differential Equations: Finite Difference Methods*, Oxford Applied Mathematics and Computing Science Series, Clarendon Press, Oxford, (1985).
11. B.J. Noye, Some explicit three-level finite-difference simulations of advection, *Mathematics and Computers in Simulation* **32** (4), 359–372 (1990).
12. B.J. Noye, Finite-difference methods for the one-dimensional transport equation, In *Computational Techniques and Applications: CTAC-87*, pp. 539–562, Elsevier Science Publishers B.V. (North-Holland), Amsterdam, (1988).
13. B.J. Noye, Finite difference techniques for partial differential equations, In *Computational Techniques for Differential Equations*, pp. 95–354, North-Holland Mathematics Studies, Elsevier Science Publishers B.V. (North-Holland), Amsterdam, (1984).
14. E.C. Du Fort and S.P. Frankel, Stability conditions in the numerical treatment of parabolic differential equations, *Mathematical Tables and Other Aids to Computation* **7**, 135–152 (1953).
15. P.J. Roache, *Computational Fluid Dynamics*, Hermosa Publishers, Albuquerque, (1972).